

Research on mechanical performances and deformation mechanism of steel irregular joint

Hu Zongbo

Institute of Equipment Management and Support, Engineering University of People's Armed Police Force, Xi'an 710086, China.

E-mail: huzongbo_1985@163.com

Abstract: According to an analysis of the mechanical behaviour of irregular joints between steel box columns and beams such as ductility, ultimate bearing capacity, degradation of strength and stiffness, energy dissipation, the deformation mechanism of the steel irregular joint panel zone is established based on the plastic hinge theory. Experimental study results indicate that irregular joints between steel box columns and beams exhibit good seismic performance and energy dissipation capacity. Ductility is consistent with the requirements of plastic ultimate deformation; bearing capacity degradation of all specimens is not significant when the displacement of the layer exceeds the ultimate displacement. Strength and stiffness degradation of all specimens are not notable when the interstory displacement exceeds ultimate displacement. The experimental results indicate that shear buckling failure in the small core area of the panel zone is the main failure mode.

Keywords: steel structure; irregular joint; degradation of strength and stiffness; mechanical performances; deformation mechanism.

1. Introduction

Beam-to-column joint is a vital part in the steel frame. Its performance can directly impact on the strength and stiffness of the whole structure. In many complex industrial and civil building structure, a lot of irregular joints are appeared. An irregular joint is defined as a joint with a beam of variable cross-section and/or a column of variable cross-section. In present years, considerable research is focused on traditional steel beam-column joints [1~4], little attention has paid to the irregular joint. Furthermore, by the variation of the beam and column section form, the force mechanism and deformation characteristics of normal joints are obviously different with irregular joints.

In this paper, through quasi-static test of six different steel box column-beam irregular joint models, some mechanical performances of steel irregular joint such as hysteretic behavior, ductility, ultimate bearing capacity, degradation of strength and stiffness, failure mechanism were studied, so as to provide reference for its design.

2. Test survey

Based on the irregular joints of the steel main workshop in a power plant, test specimens at 1/4 scale of were designed. There were two series of six cruciform joints, the JD20 series and the JD27 series. Around a joint were an identical box column but different beams, an I-shaped beam and a box beam. Welded flange and bolted web connections were used to connect the I-shaped beam and the box column; fully welded connections to connect the box beam and the box column. In order to study the shear strength of the panel zone, specimens were made according to the principle of "strong-member and weak-connection". The thickness of column web in the panel zone reduced two times [5]. Additionally, the design axial forces were, respectively, 540kN, 800kN and 1050kN. This test adopts quasi-static loading with the test setup illustrated in Fig. 1, and the materials performance of specimens shown in Table 1.

Table 1 Materials performance of steel

Plate thickness /mm	Elasticity modulus $E/10^5$ MPa	Yield stress f_y /MPa	Yield strain $\varepsilon_y/\mu\text{e}$	Ultimate stress f_u /MPa
6	2.02	310.54	1540	453.06
10	2.07	285.70	1390	430.99
12	2.07	286.35	1392	449.34

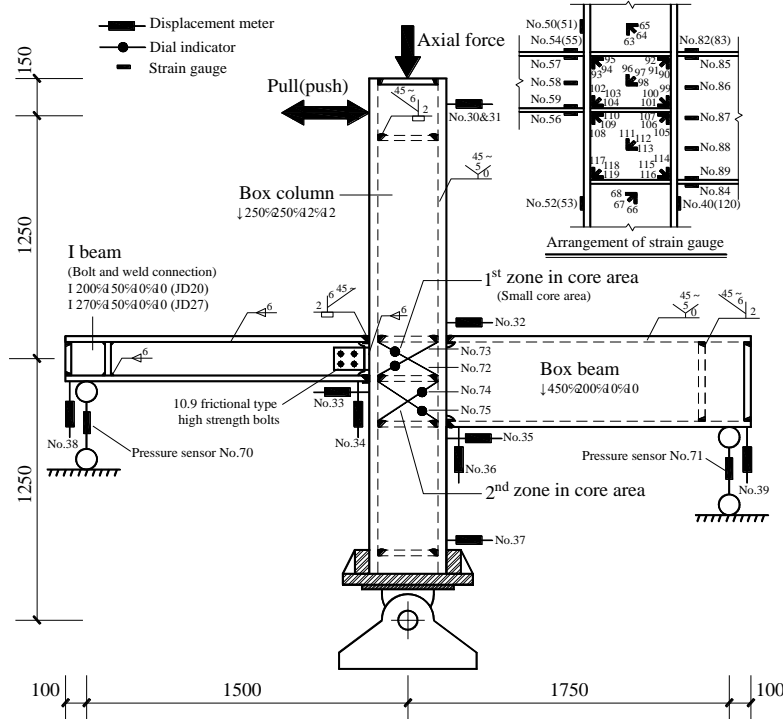


Fig.1 Specifics of the specimen

3. Analysis on mechanical performances of a steel irregular joint

3.1. Analysis on P-Δ skeleton curves

P-Δ skeleton curves of the JD20 and JD27 series are shown in Fig. 2. The following experimental results were obtained:

1) Specimens need to progress through four stages under low cycle loading, namely, elasticity, yield, limit and damage. All skeleton curves have a long declining stage, and all specimens have good ductility in the large displacement phase.

2) The box beam lower flange cannot be used to transmit tension to the panel zone, because the web weld in the 2nd zone opened, so, at that moment, only the small core area was able to bear the shear force. Therefore, the skeleton curves of the specimens sharply decline when the load exceeds the limit. The results show that the degradation of joint stiffness is significant and the residual deformation of the panel zone is increased because of the weak constraint on the 2nd zone from the box column.

3) Variation of positive load is not notable with the recession of joint stiffness in the plastic stage. However, when the load is reversed, the web weld cracks are closed under pressure from the box beam upper flange. The entire panel zone bears the shear force. At this time, degradation of joint stiffness occurs more slowly because the deformation of the joint could be constrained by the left and right beams. Consequently, the distributions of the skeleton curves are asymmetric.

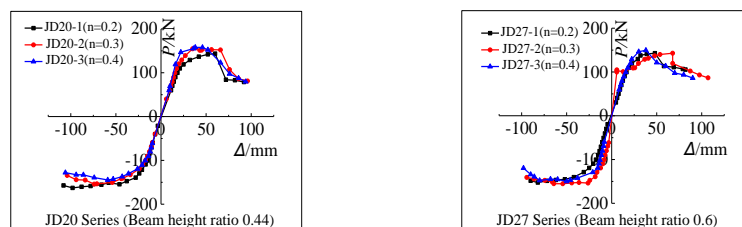


Fig. 2 P-Δ skeleton curve

3.2. Analysis on the performances of displacement ductility and energy dissipation

The results indicate that the steel box column-beam irregular joint has good seismic performance and energy dissipation capacity. As the displacement ductility coefficient of the specimen is 2.1, the deformation of the panel

zone is at the plastic stage. The displacement ductility coefficients of all specimens exceed 3, satisfying the requirements of plastic ultimate deformation. The steel irregular joint has a stronger energy dissipation capacity. Energy dissipation in the small core area of the panel zone plays a key role in the energy dissipation of the specimen. Mechanical performance parameters of the irregular joint in the steel structure are shown in Table 2.

Table 2 The performances of displacement ductility and energy dissipation

Joint number	φ_u/rad	θ_p/rad	ζ_{eq}	μ
JD20-1	0.037	0.028	0.4036	3.067
JD20-2	0.038	0.027	0.4640	3.309
JD20-3	0.038	0.022	0.4010	3.479
JD27-1	0.033	—	—	2.644
JD27-2	0.041	0.020	0.4707	3.580
JD27-3	0.036	0.028	0.4745	3.674

Note: φ_u is elastoplastic interstory displacement angle; θ_p is plastic rotation angle of the panel zone; ζ_{eq} is equivalent viscous damping coefficient; D_e is energy dissipation coefficient.

3.3. Analysis on shear deformation in the panel zone

Deformation of the panel zone is mainly shear deformation [6]. In the elastic stage, shear deformation of the panel zone is very small, almost can be ignored. But in the elastic-plastic stage, shear deformation of the panel zone increases quickly with the increase of load. As shown in the fig. 3(b), Ahead of the web weld cracking, the hysteretic curve of 2nd core area of the joint is comparatively full, but its shear deformation is obviously less than small core area. However, when the tension of bottom flange of box beam can't be passed to 2nd core area web after the web weld of 2nd core area cracking, the shear deformation of 2nd core area web is not obvious, and the shear Angle is also small. Only when the 2nd core area web bear the pressure from the bottom flange of box beam, the 2nd core area web can produce negative direction shear angle. Correspondingly, the development of hysteretic curve and the increase of shear angle of 2nd core area is along the negative direction in the fig. 3(b).

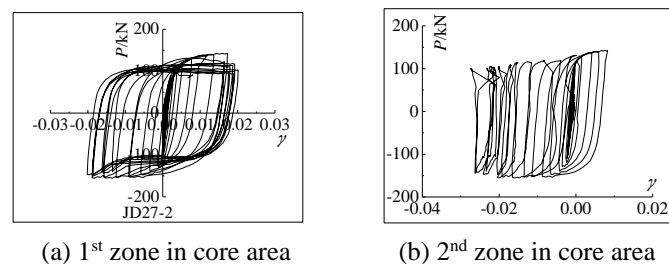


Fig.3 The hysteretic curve of column end load and rotation angle in the panel zone

3.4. Analysis on strain of panel zone

The baroclinic zone in the centre of the small core area yields first along the diagonal direction with a direction of principal stress at roughly 45°. Because the plane of the area is restrained strongly by the beam flange, the distribution of tension and compression strain in the small core area is symmetrical. Shear failure of the web in the small core area is caused by the spread of the shear yield area in the centre of the area. The entire cross-section of the small core area is plastic. At this moment, the bearing capacity of the small core area is not significantly decreased (shown in fig.4(a)), and this result indicates that the connection between the small core area clapboard and box column can transmit most of the beam end moment, similar to a plastic hinge.

Because one side of the 2nd zone is nearly free, the development of tension and compression strain along the diagonal direction is asymmetric. When the weld between the column web and column flange has been opened under reciprocating tension and compression of the box beam lower flange, the positive load of the beam end is no longer increased, because of the interrupted transmission of tension and pressure of both beams (shown in fig.4(b)). However, shear deformation of the 2nd zone web is developed in the opposite direction after closing the crack of the weld under pressure from the box beam upper flange. When the panel zone is in the plastic stage, shear deformation and capacity are no longer increased with the stagnation of the developing crack. Therefore, the connection between the box beam upper flange and the box column acts in a similar manner to a plastic hinge at the end of loading.

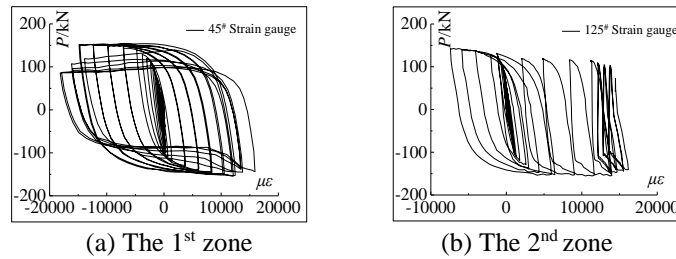


Fig.4 Strain in panel zone

Because of differences in bending moment of beam end on both sides of the joint, there is also large differences in bending stress of the left and right beam end. As shown in fig.5 (a), in each loading stage, I beam end strain along the height direction change in the linear symmetrical pattern so that shows strain distribution of the I beam end is according with flat section assumption. As shown in fig.5 (b), because the panel zone's shear transferred by top and bottom flange of box beam end are not equal, the bending stress of the box beam end change suddenly in the neutral axis of the small core area. The figure shows that the distribution of the bending stress of box beam end is linear along the height direction in the small core area. Moreover, the strain near the neutral axis and bottom flange is small within the scope of height in the 2nd zone of the core area. This is because of strain restriction by small core area. Accordingly, the strain distribution of the lower flange is basically according with flat section assumption until lower flange weld cracking, but the strain decreases after the weld crack.

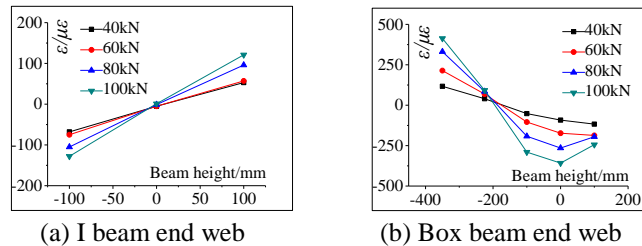


Fig.5 Strain distribution of beam end web

3.5. Analysis on strength of specimen

After specimens have entered into the plastic state, the bearing capacity of structures decrease with the increase of the number of repeated loading under the condition of constant displacement amplitude. Strength degradation coefficient λ_i is used to measure structural strength degradation in the process of all cycling at the same level [7]. In the experiment, λ_i is the ratio of same level loading cycle peak load at the last time and peak load at the first time. Under the condition of different displacement, changes in Strength degradation coefficient of all specimens are shown in table 3.

As shown in the table 3, at the early loading stage controlled by the displacement, strength degradation degree of the specimens under the condition of the same level loading is not obvious until the panel zone web weld crack. At this moment, displacement ductility coefficient of specimens is about 2.1, and strength degradation coefficient is about 0.8. This is because the shear deformation of the small core area has been restricted by the 2nd zone of core area, which reduces the speed of strength degradation. In the process of positive loading, when the displacement ductility coefficient is about 2.1, the panel zone web weld crack, the deformation of small core area suddenly increase, and bearing capacity suddenly decrease. In the late loading, development of cracks stop because of constraints of left and right beam, and the strength is slightly improved. In the process of negative loading, the panel zone always participate in the work as a whole, the 2nd zone of core area yield later than the small core area. When the damage of specimens occur in positive loading, the negative bearing capacity haven't reached the limit, so negative strength degradation curve is very smooth (shown in fig.6 (a)).

3.6. Analysis on stiffness of specimen

Degree of stiffness degradation of the specimens can directly reflect the seismic performance of structural components. Namely, under the condition of constant displacement amplitude, the characteristic of stiffness decrease of structural components with the increase of the number of repeated loading is called the stiffness degradation [7]. The secant stiffness of the same level deformation is used to represent the degree of stiffness degradation. In this test, secant stiffness under a certain level load displacement take the average of the three circulation secant stiffness at the same level. The calculation results of secant stiffness are shown in table 4.

The fig.6 (b) shows that the stiffness of joints have degraded quickly before the displacement ductility coefficients of specimens have reached 2.1. But after the specimens have completely gotten into the plastic, stiffness degradation curves of six joints are smooth, and then the beam end has produced plastic hinge. As can be seen from the overall trend of the stiffness degradation, joint stiffness constantly degrades with the increase of load displacement. The root cause of stiffness degradation is elastoplastic properties and accumulated damage after the joint yield. Beam height ratio significantly impact on the secant stiffness of the specimens. As shown in the figure, secant stiffness of JD27 series specimens is greater than JD20 series specimens, and stiffness degradation speed of JD27 series specimen is faster than JD20 series specimen. The axial compression ratio also has effect on secant stiffness of specimens, and stiffness degradation speed of specimen JD20-3 and JD27-3 which has larger axial compression is faster than other specimens. This shows that additional bending moment caused by second-order effect (N-Δ effect) has significant influence on joint’s plastic deformation with the increase of the horizontal displacement when the axial compression is larger. Which further increase the accumulated damage after the joint yield [8].

Table 3 Strength degradation coefficient

μ_y	Strength degradation coefficient λ_i						
	JD20-1	JD20-2	JD20-3	JD27-1	JD27-2	JD27-3	
+	1.4	1.012	1.033	1.007	1.023	1.006	0.912
	1.8	0.994	1.014	0.926	0.833	1.011	0.771
	2.1	0.787	0.723	0.817	0.975	0.838	0.866
	2.5	0.857	0.83	0.938	0.965	0.885	0.973
	2.9	0.952	0.986	0.946	0.98	0.923	0.966
-	-1.8	0.937	1.002	0.987	0.988	0.997	1.033
	-2.1	0.973	0.999	0.986	0.972	0.992	0.982
	-2.5	0.97	0.947	0.944	0.965	0.955	0.987
	-2.9	0.985	0.93	0.972	0.971	0.957	0.936
	-3.2	0.993	0.929	0.979	0.945	0.965	0.966

Table 4 Secant stiffness

μ_y	θ_p	Secant stiffness K_i /kN/mm					
		JD20-1	JD20-2	JD20-3	JD27-1	JD27-2	JD27-3
1.4	0.017	3.965	2.98	2.929	3.458	4.195	3.362
1.8	0.021	3.208	2.512	2.19	2.618	3.422	2.514
2.1	0.018	2.251	1.448	1.684	2.123	2.504	1.925
2.5	0.017	1.713	1.252	1.383	1.814	1.869	1.658
2.9	0.018	1.36	1.248	1.18	1.589	1.465	1.445

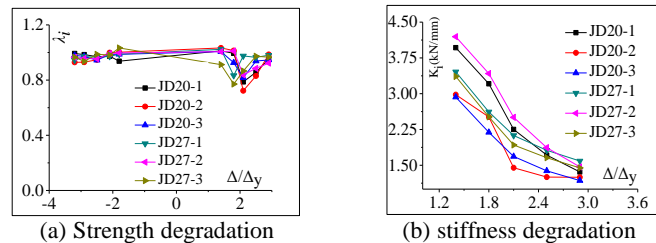


Fig.6 Strength degradation curves and stiffness degradation curves

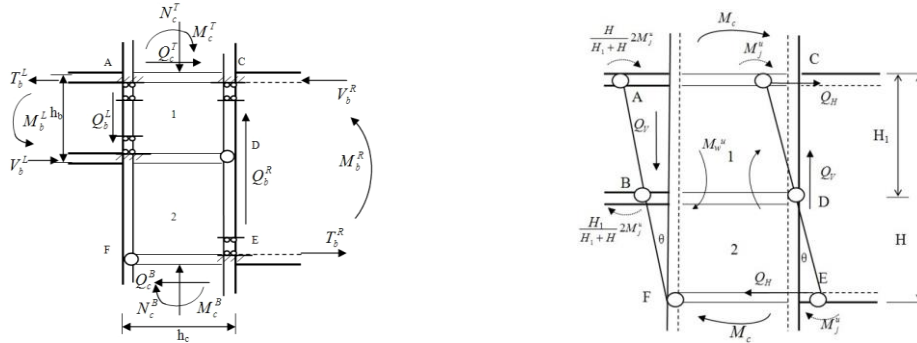
3.7. Establishment of the deformation mechanism

The experimental results indicate that shear buckling failure in the small core area of panel zone is the main failure mode. Horizontal shear deformation in the small core area has been generated as a result of the shear force transmitted from the upper clapboard, the lower clapboard, and the connection between the inner clapboard and the box column. Most of the beam end moment was still transmitted when the whole cross-section of the small

core area was in a plastic state [9]. Therefore, the shear deformation mechanism of the small core area can be considered to approximate the mechanism resulting from inner clashboard fixed in the vertical direction as a load-bearing hinge.

Because the weak side of the 2nd zone cannot bear the beam end moment along with the small core area, the connection between the inner clashboard and the box column cannot effectively transmit the beam end moment after the 2nd zone yield. Therefore, the small core area and 2nd zone cannot resist the shear deformation as a whole panel zone. Consequently, the shear deformation mechanism of the 2nd zone can be considered to approximate the mechanism resulting from the inner and middle clashboards of the free end being completely hinged with the flange of the column.

To sum up, the mechanical model of an irregular joint between a steel box column and beam is shown in fig.7 (a). At the beginning of the yield stage, assume that the moment transmitted by the directional hinge bearing is proportional to the height of the panel zone. The entire shear deformation mechanism of the panel zone is shown in fig.7 (b).



(a) Mechanical model of an irregular joint (b) Deformation mechanism of the panel zone
Fig.7 Deformation mechanism of a steel irregular joint

As shown in fig.7, the whole section of the panel zone is plastic, the bending deformation of the beam end is considered, and the axial deformation of the diaphragm is ignored. Based on the virtual work principle [10], the following formula is established.

$$-Q_H h_b \theta = -2M_c \theta + Q_v h_c \theta = -4M_w^u \theta - 4M_j^u \theta \quad (1)$$

where M_w^u is the plastic bending capacity of the whole web cross section caused by the beam bending deformation; M_j^u is the plastic bending capacity of the whole cross section in the connection between the small core area diaphragm and the column; M_c is the average moment of upper and lower column; t_p and t_w are the thickness of the inner diaphragm of the column and the web, respectively. f_{yw} and f_{yp} are the yield strength of the inner diaphragm and web in the panel zone, respectively; Q_H and Q_V are the average values of horizontal shear and beam end shear, respectively.

4. Conclusions

Based on the experimental and theoretical study results, the conclusions summarized are as follows:

1) The displacement ductility coefficient μ of six joint specimens is 2.02 between 2.66, with a mean of 2.29. The displacement ductility coefficients of six joint specimens is not very big. The reason is that bearing capacity drops rapidly because of sudden fracture of the weld between steel column flange and connection web under the action of repeated horizontal load after the web of joint core area yield. Therefore, the weld quality of the panel zone is highly valued.

2) Shear deformation is the main deformation mode in the panel zone. Because of uncoordinated deformation between 1st zone of core area and 2nd zone of core area, the development of shear angle of 2nd core area is only along the negative direction. Under the reciprocating loading on the column end, tension and compression strain along the diagonal direction of the core area develop rapidly, and small core area yield first. In the each loading stage, the strain of beam end and column end is very small.

3) After joints yield, the specimens occur degradation phenomenon of strength and stiffness. When specimens completely get into the yield state, the degradation of strength and stiffness is obvious. With the increase of height of the small core in the panel zone, energy dissipation capacity of panel zone is slightly increased. The greater the axial compression ratio increase, the more amplitude the bearing capacity decrease. In general, steel

irregular joints have the same failure characteristics with other normal steel joints, and have good late deformation ability and better seismic performance.

4) The experimental results indicate that shear buckling failure in the small core area of the panel zone is the main failure mode. And the deformation mechanism of the steel irregular joint panel zone between the steel box column and beam is established based on the plastic hinge theory.

5. Acknowledgments

The financial assistance provided by the Natural Science Foundation of China No. 51308444 and the Postdoctoral Science Foundation of China No. 20080440814. These supports are gratefully acknowledged.

6. References

- [1] Krawinkler H., Popov E. P.. Seismic behavior of moment connections and joints. *Journal of the Structural Division*, 108(ST2), 373-391.
- [2] Popov E. P., Pinkney R. B.. Seismic moment connections for MRFs. *Journal of the Structural Division*, 10(1-4), 163-198.
- [3] Krawinkler H.. Shear in beam - column joints in seismic design of steel frames. *Engineering Journal*, 66(1), 82-91.
- [4] Tsai K. C.. Steel beam-column joints in seismic moment resisting frames. Ph.D. dissertation, Department of Civil Engineering, University California, Berkeley, Calif.
- [5] Hu Z. B.. Experimental and theoretical research on performance of irregular joint between steel box columns and beams. Xi'an University of Architecture and Technology, Xi'an. (in Chinese)
- [6] Mulas M. G.. A structural model for panel zones in nonlinear seismic analysis of steel moment-resisting frames. *Engineering Structures*, 26(2), 363-380.
- [7] Wang W. Z.. Fracture mechanism, cyclical performance and design recommendations of welded flange-bolted web beam-to-column rigid connections in steel moment frames under seismic load. Xi'an University of Architecture and Technology, Xi'an. (in Chinese)
- [8] Xue J. Y., Hu Z. B., Peng X. N., Liu Z. Q. Analysis of shear resistance of irregular joint between steel box columns and beams. *Civil Engineering Journal*, 44(8): 9-15. (in Chinese)
- [9] Chen S. F.. Principles of steel structure design. Science and Technology Press, Beijing, 188-189. (in Chinese)
- [10] Wardenier J.. Hollow Section in Structural Applications. John Wiley & Sons, New York.